# Détection de Structures Cohérentes dans des Écoulements Fluides et Interfaces Homme-Machine pour l'Exploration et la Visualisation Interactive de Données Scientifiques.


Thèse réalisée par Florimond Guéniat,

sous la direction de M. Ammi, F.Lusseyran et L. Pastur


06 Décembre 2013


PARIS-SUD University - LIMSI

Orsay, FRANCE

# Hydrodynamic systems

Both open and confined flows are complex, and has potentially an infinite number of DoF, but coherent structures seem to play a major role.

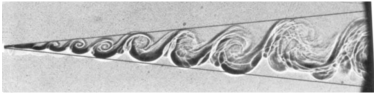

Brown & Roshko, (1974), *J. Fluid Mech.*

What is a coherent structures (see *e.g.* Chassaing, Hussain, Lumley ...) ?

- spatially localized
- significant contribution to the kinetic energy
- significant life-time
- recurrent phenomenon
- material frontiers
- etc.

Von 'Heartman' street
Isla Socorro ($Re > 10^{10}$ !).

*"In principle, concepts like coherent structures are best left implicit."*

Hussain, (1986) *Phys. Fluids.*

Several relevant frameworks exist to identify coherent structures.

# Lagrangian framework


Eruptions of Eyjafjallajökull. Estimated ash cloud on 15 April 2010.

In fluid mechanics :

$$\dot{\mathbf{X}} = \mathbf{u}\left(\mathbf{X}, t\right)$$

with $\mathbf{X} \in \mathcal{R}^3$

**u** comes from DNS or PIV measurement.

$\nabla \cdot \mathbf{u} = 0$ implies the system is conservative (within dynamical system frame).

If the system is autonomous or periodic, then the dynamic is driven by invariant manifolds.

# Lagrangian framework

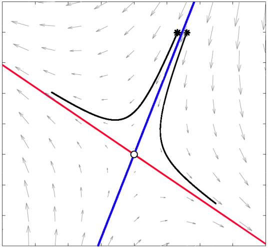

In autonomous system, stable and unstable manifolds :

- are attached to a fixed point
- are invariant
- are material frontiers
- are edges of invariant sets
- drive transport and mixing
- are hyper planes of locally maximum stretching

# Modal framework

The aim is to give a relevant representation of a dataset, *e.g.* the energy (POD) or the frequencies (Fourier).

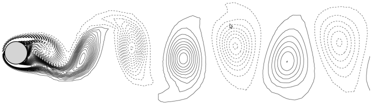

Cylinder wake

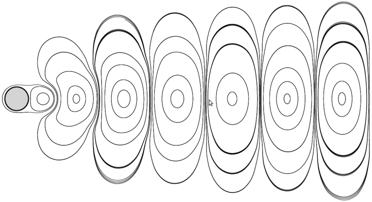

POD mode 1

Bergmann & Cordier, (2008) *J. Comput. Phys.*

# Modal framework

The aim is to give a relevant representation of a dataset, *e.g.* the energy (POD) or the frequencies (Fourier).

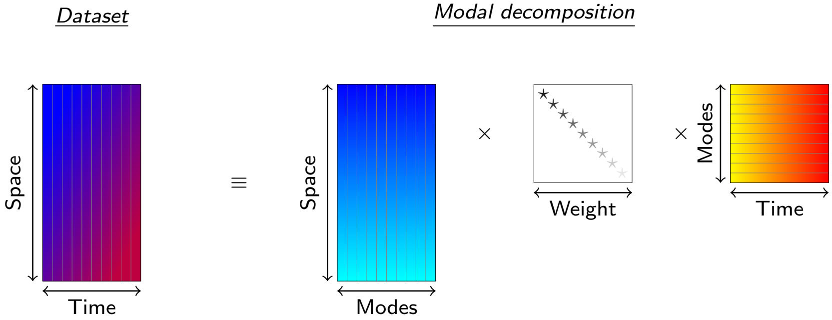


It may lead to model reduction, through Galerkin-projection or truncature.

# Big data

## Understand fluid mechanics

- Numerous fields/points of view
  - Velocity
  - Pressure
  - Temperature
  - Concentration ...
- Large 3DnC simulations
- Hi-Res experimental snapshots

## Leads to huge dataset

- number of points : $c \times n^d \times N$

with typically

| | c | d | N | n |
|---|---|---|---|---|
| DNS | 5 | 3 | 1000 | 124 |
| Exp | 2 | 2 | 10000 | 1000 |

How to interactively visualize such a dataset ?

# Big data

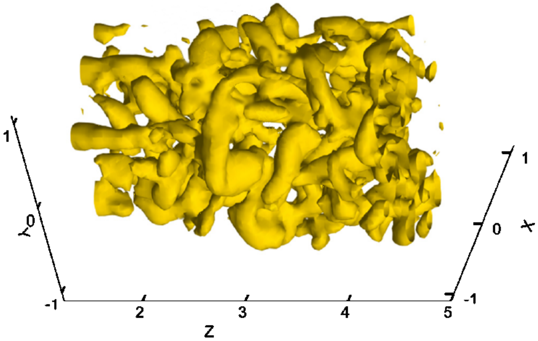


Violatoa & Scarano, (2011) *Phys. Fluids*

How to interactively visualize such a dataset ?

# A question as old as the notion of coherent structure

*" Prejudices which are essential for the success of a coherent structure study, can also become liabilities as these can easily mislead one ; one can usually see in flow visualization what one wants to see as one can find different structures in the same signal ."*

Hussain, (1983) *Phys. Fluids.*

# A question as old as the notion of coherent structure

*" Prejudices which are essential for the success of a coherent structure study, can also become liabilities as these can easily mislead one ; one can usually see in flow visualization what one wants to see as one can find different structures in the same signal ."*

Hussain, (1983) *Phys. Fluids.*

# Illusion from sensitivity

The same data (a 2D gaussian), plotted with 3 different color map.

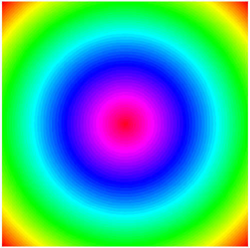

Rainbow

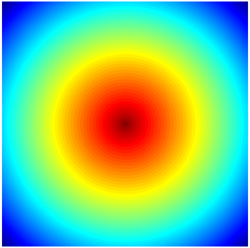

Jet

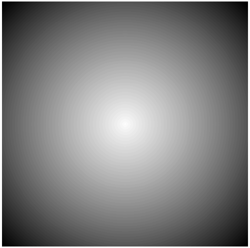

Gray

How to be sure an expert correctly discriminates and interprets signals ?

# Outline

- Introduction
- Presentation of the cavity flow

- Spectral decomposition of a dataset
  - Dynamic Mode Decomposition
  - Non-Uniform DMD
- DMD-Observability
- Lagrangian Coherent Structures
  - Identifying Material Frontiers
  - Fastening the algorithm

- Interactive exploration of scientific dataset
- Discrimination between multidimensional stimulus

- Conclusion and openings

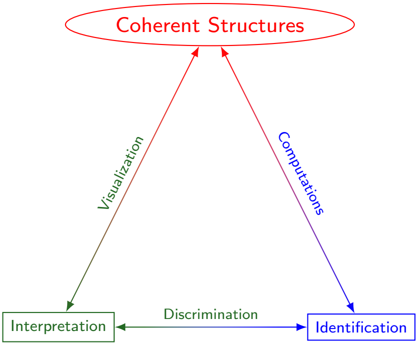

– Cavity flow –

# Cavity flow

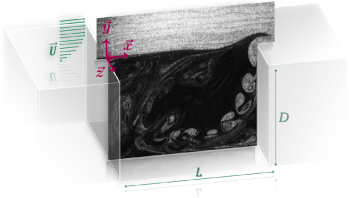


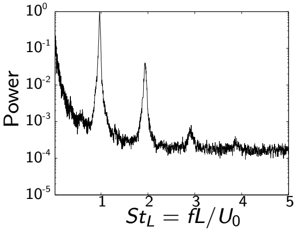


This frequency corresponds to the selected shear layer instability.

– Dynamic Modes Decomposition (DMD) –

# What are dynamic modes ?

Schmid [1] ; Rowley [2] ;
→ Assume there exists an operator of evolution, $A$, such as the $\mathbf{u}_k$ are realisations of a *nonlinear* process.

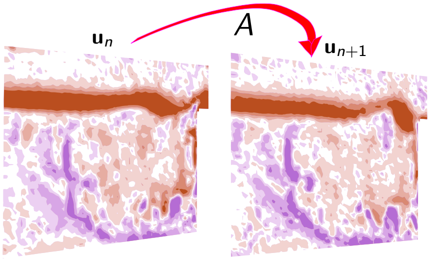


→ Find a similar matrix to $A$. *Dynamic modes are defined as eigenvectors of A*, computed thanks to the similar matrix.

1. Schmid *et al* (2008) *66th APS meeting* ; Schmid, (2010) *J. Fluid Mech.*
2. Rowley *et al*, (2009) *J. Fluid Mech.*

# Defining the Evolution Operator $A$ [BIFD2013a]

If $\phi$ is the flow of the fluid dynamical system :

$$\mathbf{X}_{n+1} = \phi_{\Delta t}\mathbf{X}_n,$$

and $\Pi$ is the projector onto the experimental space (*i.e.* $\mathbf{u}_n = \Pi\mathbf{X}_n$), $A$ is defined by :

$$A \circ \Pi = \Pi \circ \phi_{\Delta t}.$$

Then,

$$\begin{aligned} A\mathbf{u}_n &= A \circ \Pi\mathbf{X}_n \\ &= \Pi \circ \phi_{\Delta t}\mathbf{X}_n \\ &= \Pi\mathbf{X}_{n+1} \\ &= \mathbf{u}_{n+1} \end{aligned}$$

# How to compute a similar matrix ?

The dataset is $K_1^{N+1} = \{\mathbf{u}_1, \dots, \mathbf{u}_{N+1}\}$.
With $\mathbf{u}_{N+1} = \mathbf{u}_1 s_1 + \dots + \mathbf{u}_N s_N + \epsilon$, then :

$$AK_1^N = K_2^{N+1} \approx K_1^N S.$$

It follows :

$$S = \begin{pmatrix} 0 & 0 & \dots & 0 & s_1 \\ 1 & 0 & \dots & 0 & s_2 \\ 0 & 1 & \dots & 0 & s_3 \\ \vdots & & \ddots & & \vdots \\ 0 & 0 & \dots & 1 & s_N \end{pmatrix}$$

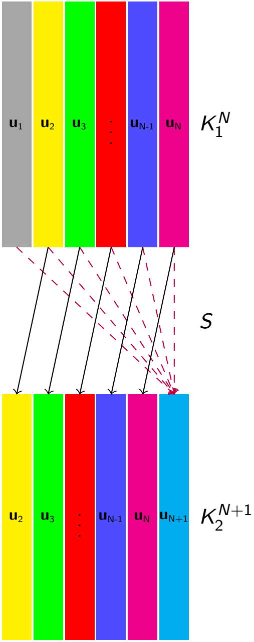

# How to compute DMD modes ?

Eigenvalues of $S$ are eigenvalues of $A$.

Let $\nu$ be an eigenvector associated with the eigenvalue $\lambda$ :

$$\begin{aligned} AK_1^N\nu &= K_1^N S\nu \\ &= K_1^N \lambda\nu \\ A\left(K_1^N\nu\right) &= \lambda\left(K_1^N\nu\right) \end{aligned}$$

Eigenvectors $\mathbf{\Phi}$ of $A$ are derived from eigenvectors $\nu$ of $S$ : $\mathbf{\Phi} \equiv K_1^N \boldsymbol{\nu}$

They are named *Dynamic modes*.

– DMD Properties –

# Spectral properties of DMD

When expressing a snapshot on the eigenspace of $A$ :

$$\begin{aligned} \mathbf{u}_n &= A\mathbf{u}_{n-1} \\ &= A\sum_i a_i^{n-1}\mathbf{\Phi}_i \\ &= \sum_i a_i^{n-1}\lambda_i\mathbf{\Phi}_i, \end{aligned}$$

so, by recurrence :

$$\mathbf{u}_n = \sum_i a_i^1\lambda_i^n\mathbf{\Phi}_i \equiv \sum_i \lambda_i^n\mathbf{\Phi}_i,$$

# Spectral properties of DMD

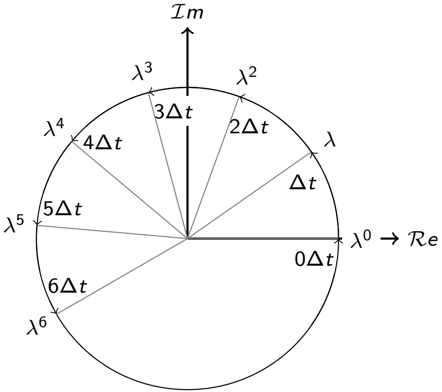


which means :

$$\lambda = \rho \exp\left(\sqrt{-1}\omega \Delta t\right).$$

# Rewriting the DMD

From this, Chen *et al.*[3] proposed a new writing of DMD

$$K_1^N = M \times V$$

where : $V = \begin{pmatrix} \lambda_1^1 & \lambda_1^2 & \dots & \lambda_1^N \\ \lambda_2^1 & \lambda_2^2 & \dots & \lambda_2^N \\ \vdots & \vdots & \ddots & \vdots \\ \lambda_{N_{\text{md}}}^1 & \lambda_{N_{\text{md}}}^2 & \dots & \lambda_{N_{\text{md}}}^N \end{pmatrix}$, and : $M = \left\{ \mathbf{\Phi}_1, \dots, \mathbf{\Phi}_{N_{\text{md}}} \right\}$.

- $N_{\text{md}}$ : number of modes
- $N$ : number of snapshots

3. K. Chen *et al.*, (2012) *J. Nonlinear Sci.*

# DMD power-like spectrum

A power-like spectrum can be constructed on $f = \frac{\mathcal{I}m(\log(\lambda/\rho))}{2\pi\Delta t}$ and $\|\mathbf{\Phi}\|$

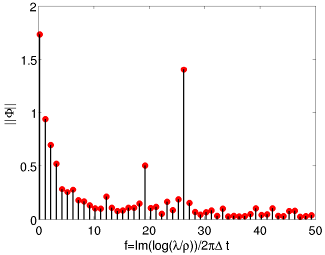

– Comparison of 2D and 3D dynamic modes of the cavity flow –

# Shear layer DMD mode [BIFD2013a]

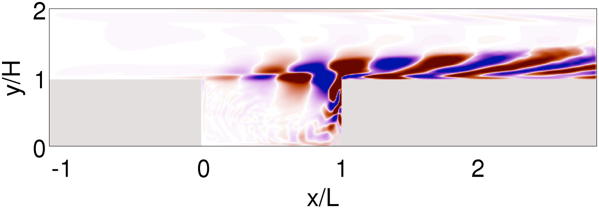


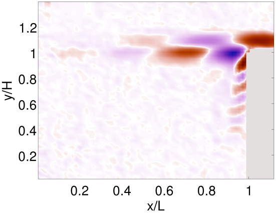

# Shear layer DMD mode[BIFD2013a]

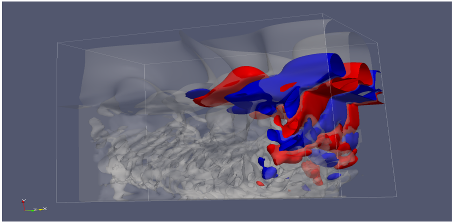

# – Sampling constraint –

# DMD and uniform sampling

The DMD algorithm needs an uniform sampling.

$$AK_1^N \equiv \{A\mathbf{u}_1, A\mathbf{u}_2, \ldots, A\mathbf{u}_N\} = \{\mathbf{u}_2, \mathbf{u}_3, \ldots, \mathbf{u}_{N+1}\} \equiv K_2^{N+1}$$

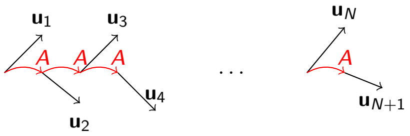

# DMD and uniform sampling

## Data problems

- Corrupted dataset
- Incomplete dataset
- Convergence of data pre/post-treatment

uniform sampling is not always possible

## Experimental problems : example taken in Fluid Mechanics

Observable :
2D2C field (PIV) $\rightarrow 1000 \times 1000px$
Frequencies of the flow :

1. one low ($\approx 0.1Hz$) $\Rightarrow$ $10s$ of sampling at least
2. one high ($\approx 200Hz$)$\Rightarrow$ sampling rate at $400Hz$

Depth of images : 12-bit
Broad-band needed :
$bb = 400 \times 1000^2 \times 12 > 4Gb.s^{-1}$
for at least $10s$

*Unreachable for standard material*

– Non-Uniform DMD –

# Non-Uniform DMD [ICTAM2012]

With the expression

$$\mathbf{u}_n = \sum_j a_i^1 \lambda_j^n \mathbf{\Phi}_i \equiv \sum_j \lambda_j^n \mathbf{\Phi}_i,$$

we can write more generally :

$$\begin{array}{lclcl} \mathbf{u}_{t_n} & = & \sum_j \lambda_j^{t_n} \mathbf{\Phi}_j + \mathbf{e} & \approx & \lambda_1^{t_n} \mathbf{\Phi}_1 + \lambda_2^{t_n} \mathbf{\Phi}_2 + \dots \\ K & = & M\,V + R & \approx & M\,V. \end{array}$$

# How to achieve this decomposition ?

$$K = M\,V + R \approx M\,V.$$

## Pseudo-Vandermonde Matrix and Modes

$V$ [4] is :

$$V = \begin{pmatrix} \lambda_1^{t_1} & \lambda_1^{t_2} & \dots & \lambda_1^{t_N} \\ \lambda_2^{t_1} & \lambda_2^{t_2} & \dots & \lambda_2^{t_N} \\ \vdots & \vdots & \ddots & \vdots \\ \lambda_{N_{\mathrm{md}}}^{t_1} & \lambda_{N_{\mathrm{md}}}^{t_2} & \dots & \lambda_{N_{\mathrm{md}}}^{t_N} \end{pmatrix},$$

and $M$ is the modes :

$$M = \begin{pmatrix} \psi_1 & \dots & \psi_{N_{\mathrm{md}}} \end{pmatrix}.$$

4. times $t_i$ are taken arbitrary, not necessary ordered.

# How to achieve this decomposition ?

## Obtaining of the Spatial Modes

Matrix $M$ is easily computed :

$$M \approx K\,V^{+},$$

where $V^{+}$ is Moore-Penrose pseudo-inverse of $V$.

## Obtaining the frequencies

$M$ can be switched in equation $K = M\,V + R$. Then :
$K \approx K\,V^{+}\,V + R$.

$V$ can be computed by minimizing the residue matrix $R$[5] :

$$R \approx K\,\left(\mathcal{I} - V^{+}\,V\right).$$

The modes follows immediately through $M \approx K\,V^{+}$.

5. K. Chen *et al.*, J. Nonlinear Sci. 22.6 (2012).

# Illustration [ICTAM2012]

$St_L = 1.02$

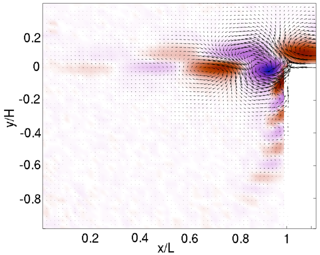


DMD mode
500 snapshots

$St_L = 1.02$

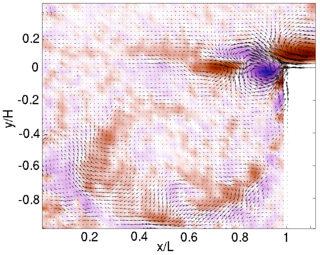


NU-DMD mode
12 randomly taken snapshots

– DMD-Observability –

If we consider an time series $\tilde{\mathbf{u}}$ extracted from $\mathbf{u}$ [6] , we can write the automatic system :

$$\left\{ \begin{array}{lcl} \mathbf{u}_{n+1} & = & A\mathbf{u}_n \\ \tilde{\mathbf{u}}_n & = & C\mathbf{u}_n \end{array} \right. ,$$

Then the system is observable ($\mathbf{u}_0$ can be reconstructed from the $n_p$ first $\tilde{\mathbf{u}}$) if the Kalman matrix have a full rank :

$$\mathcal{K} = \begin{pmatrix} C \\ CA \\ \vdots \\ CA^{n_p-1} \end{pmatrix}.$$

Practically, the conditioning of $A^i$ is blowing up, so it is undoable to estimate the observability qualities of time series with the Kalman Matrix.

6. where $\mathbf{u} \in \mathcal{R}^{np}$

*" When you think about a variable, the evolution of it must be influenced by whatever others variables it's interacting with. Their values must somehow be contained in the history of that thing. Somehow their mark must be there. "*

James Farmer, (1986) *Interview with James Gleick*

J.D. Farmer *et al.*, "Geometry from a time series", (1980), *PRL*

*" When you think about a variable, the evolution of it must be influenced by whatever others variables it's interacting with. Their values must somehow be contained in the history of that thing. Somehow their mark must be there. "*

James Farmer, (1986) *Interview with James Gleick*

J.D. Farmer *et al.*, "Geometry from a time series", (1980), *PRL*

# Propagation of the field

$\mathbf{u}_{n+1} = A\mathbf{u}_n$ :

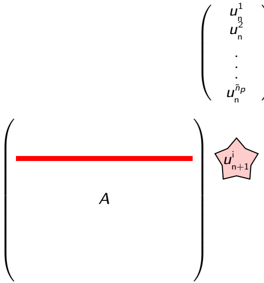


The number of elements on the $i$th line allows to count points influential in the dynamics of the observable $\{u^i\}$

# DMD-observability criterion [RNL2013]

Then, by counting the number of significant components of $A$ :

- $n_l$ on the $i$th line
- $n_c$ on the *ith* column

we define the DMD-observability for the $i$th component as :

$$\sigma_\alpha(i) = \frac{1}{n_p}\left(\alpha n_l + (1-\alpha)(n_p - n_c)\right)$$

We can approximate the operator $A$, thanks to the DMD algorithm :

$$A \approx K_1^N S K_1^{N^{-1}}.$$

– Illustration –

# Toy examples

If we take a synthetic matrix $A \in \mathcal{M}_n$, and a random vector $v \in \mathcal{M}_{n,1}$, we can construct a synthetic dataset :

$$K_1^N = \left\{ A \times v, A^2 \times v, \ldots, A^N \times v \right\}$$

# Toy examples

If $A$ is :

$$A = \begin{pmatrix} 1 & 0 & 0 & 1 & 1 \\ 0 & 1 & 0 & 0 & 0 \\ 1 & 0 & 1 & 1 & 1 \\ 0 & 0 & 0 & 1 & 1 \\ 1 & 0 & 0 & 1 & 0 \end{pmatrix}$$

then :

| Component : | 1 | 2 | 3 | 4 | 5 |
|---|---|---|---|---|---|
| Rank of $\mathcal{K}$ | 3 | 1 | 4 | 3 | 3 |
| $\sigma_{0.5}$ | 0.48 | 0.44 | 0.60 | 0.50 | 0.47 |

# Illustration on a cavity flow [RNL2013]

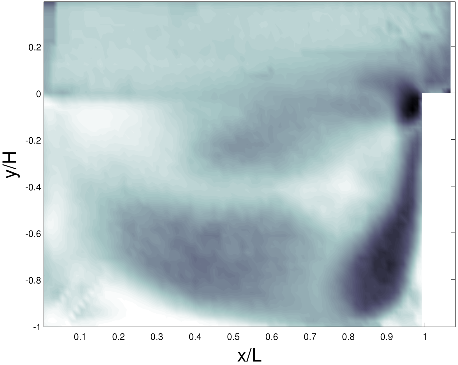


Good agreement with experimental placement of sensors and with Basley [7] .

7. J. Basley, 2012, *PhD thesis*

# – Identification of Lagrangian Structures –

# Material frontier

Dynamical flow : $\vec{\mathbf{X}}(t) = \phi^t\left(\vec{\mathbf{X}}(0)\right)$
Invariant manifolds are invariant through the flow.
Consequently : such a manifold is a material frontier.

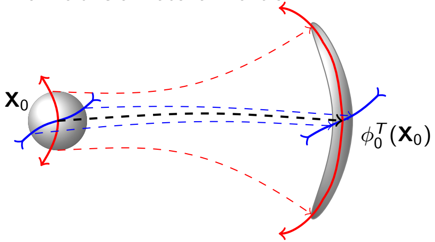


temps : $t = 0$ temps : $t = T$

# Stretching of fluid particles

*How to identify these manifolds ?*

Fluid particles are deformed by manifolds.

Miller *et al.*[8] and Haller *et al.*[9] had proposed to look at the stretching of fluid particles.

$$\delta X(T) = \frac{\mathrm{d}\phi^T(X)}{\mathrm{d}X}\delta X(t_0) = J\delta X(t_0)$$

8. Miller *et al.*, (1997) *Physica D*
9. Haller *et al.*, (1998) *Physica D*, (2000) *Chaos*, (2005) *J. Fluid Mech.*

# Cauchy Green Tensor

Quantifying the stretching is done by the evaluation of the Cauchy Green Tensor [10] :

$$\mathbf{C} = J \times J^{\dagger}$$

Then, the particule deformation rate is driven by the maximum eigenvalue of **C**, *i.e.* Finite-Time Lyapunov Exponent of the flow [11] .

10. Haller *et al.*, (1998) *Physica D*, (2000) *Chaos*, (2005) *J. Fluid Mech.*
11. S.C. Shadden,*et al.*, (2005) *Physica D*

# Lagrangian Coherent Structures

In autonomous/periodic system : invariant manifolds create ridges in the FTLE field.

In non autonomous system, there is non uniqueness of manifolds. Nevertheless, the ridges are still (most of the time) material frontier, and drive the mixing.

Ridges are called *Lagrangian Coherent Structures*.

– High Performance Computing –

# Issues in computing FTLE fields [BIFD2011,2013b]

## BottleNecks

1. Numerous particles.
2. SIMD implies Cartesian Grid, i.e. space increment has to be constant.
3. Elementary flow interpolation is time consuming.

## Implemented solutions

1. SIMD – vectorization (x100).
2. Conformal transformation of the dataset.
3. Interpolation on GPU. (x100)

# Time-independent computations [BIFD2011,2013b]

Trajectory in physical space $\equiv$ composition of elementary flow map [12] [13] .

$$\phi_{t_A}^{t_C}\left(\mathbf{X}\left(t_A\right)\right)=\mathbf{X}\left(t_C\right)$$

with

$$\phi_{t_A}^{t_C}=\phi_{t_B}^{t_C}\circ\phi_{t_A}^{t_B}$$

When constructing a collection of elementary flow maps $\left\{\phi_{t_i}^{ti+1}\right\}$, each elementary flow map may be computed with no time dependence.

12. S.L. Brunton and C.W. Rowley, (2010) *Chaos*
13. K. Giest *et al.*, (1990) *Theoretical Physics*

# Illustration

Attractive (red), repulsive (blue) LCS and vorticity field.

– Interactive exploration of a dataset –

*“ The purpose of computing is insight, not numbers. ”*

Richard Hamming, (1962) *Numerical Methods for Scientists and Engineers*

*“ Getting information from a [matrix] is like extracting sunlight from a cucumber. ”*

Arthur and Henry Farquhar, (1891) *Economic and Industrial Delusions*

# Interfaces for Scientific Visualization

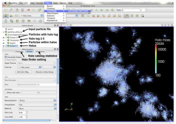
J. Woodring (2011)

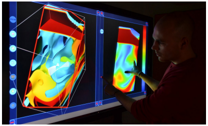
P. Isenberg (2013)

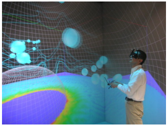
N. Ohnoa & A. Kageyama (2010)

Desktop [14] – 2D interaction

Tactile device [15] – colocalized interaction

CAVE [16] – immersive and 3D interaction

14. J. Woodring *et al.*, (2011) *The Astrophysical Journal Supplement Series*
15. P. Isenberg *et al.*, (2013) *Computer Graphics and Applications*
16. N. Ohnoa & A. Kageyama, (2010) *European Union symposium on Ambient intelligence*

# Key points for Interactive Visualization of Scientific Dataset

User-centered design : Field study and field experiment [17]

## Primary features

- Six DoFs exploration
- Several interaction modes
  - Cutting plane
  - Isosurfaces
  - Switch between quantities
  - Streamlines
  - *etc.*

## Secondary features

- Easy to use
- Collaborative-friendly
- Portable interface
- Easy to spread (*i.e.* cheap)

17. Carpendale, (2008) *Information Visualization*

*"Today, 3D interaction in games, CAD, or 3D animation applications is performed mainly with the 2D mouse."*

Bernd Froehlich, (2008) *Comput. Graph. Appl.*

# Tangible interfaces for Scientific Visualization

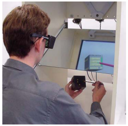
Martens (2004)

Benefits of Tangibles :

- manipulate the data/the scene [18] [19]
- interact with the data [20]
- sense of touch [21]
- colocalized data and interaction [22]

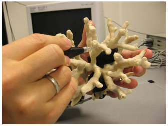
Kruszyński (2009)

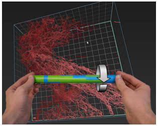
Jackson (2013)

18. Shaer & Hornecker, (2010) *Found. and Trends in H-C Interaction*
19. Jackson *et al.*, (2013) *Trans. Visual. Comput. Graphics*
20. Martens *et al*, (2004) *European Union symposium on Ambient intelligence*
21. Fitzmaurice *et al.*, (1995) *SIGCHI conference on Human factors in computing systems*
22. Kruszyński & Van Liere, (2009) *Virtual reality*

# Expected benefits for the Visualization of Dataset

- Intuitive metaphor
  1. increase of interaction transparency
  2. better reactivity
  3. shorter training phase
- Strong parallax effects $\rightsquigarrow$ better depth perception **without** a stereoscopic device

# Seeing the dataset through a tablet [VRST2013]

A tablet is considered as a moveable window to a virtual world [23] [24] .

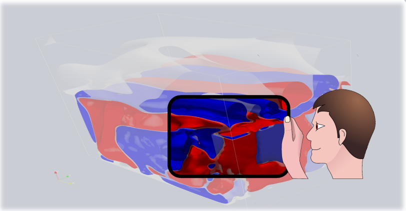

A displacement of the tablet results to a displacement of the camera in the scene.

23. Scarpa, *et al.*, (2006) *Future Gen. Comp. Sys.*
24. Tsang, *et al.* (2002) *15th ACM symp. on User interf. soft. and tech.*

# Illustration

Navigation with a tangible window

# Illustration

Use of a reference tangible

Use of a tangible tool

– Tangible metaphors evaluation –

# Evaluation

## Primary features

- Six DoFs exploration - **H1**
- Several interaction modes
  - Cutting plane - **H2**
  - Isosurfaces
  - Switch between quantities
  - Streamlines
  - *etc.*

## Secondary features

- Easy to use - **H3**
- Collaborative-friendly
- ✓ Portable interface
- ✓ Easy to spread (*i.e.* cheap)

**H1,H2,H3** : working hypothesis

# Navigation : Windows in hand [VRST2013]

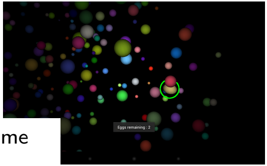


Task : find "eggs" (target) in a galaxy of spheres.

Spatial displacement over time

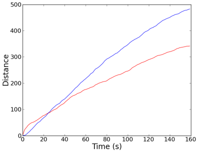


Angular displacement over time

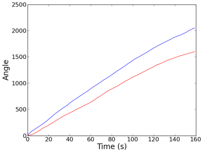


-**C1** : tangible window
-**C2** : touch screen

| | Widget activation | Mean velocity | Motionless |
|---|---|---|---|
| Comparison **C1/C2** | +98% | +32.2% | −40.6% |

With the window metaphor, users travel more in the scene, in less time. They actually **know** where to go.

These results are statistically significant ($p \ll 0.01$) in favor of the Window metaphor.

- **H1** is validated

# Navigation : Windows in hand [VRST2013]

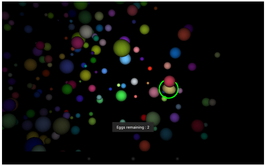


Subjective measures :
-**MS1** : Rotating in the scene
-**MS2** : Finding their way – Difficulty to self-localization

| Measure : | **MS-1** | | **MS-2** | |
|---|---|---|---|---|
| conditions | **C1** | **C2** | **C1** | **C2** |
| Median | 4.0 | 3.0 | 4.0 | 3.0 |
| p-value : | $p = 0.012$ | | $p = 0.037$ | |

These results are statistically significant ($p \ll 0.01$) in favor of the Window metaphor.

- **H3** is validated

# Navigation : Manipulation [25] of the dataset

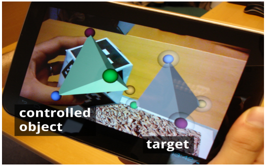


Task : dock a virtual objet in a target position.

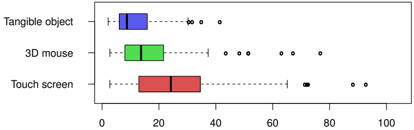


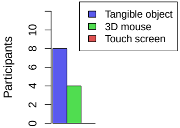


All these results are highly statistically significant ($p < 0.01$) in favor of the tangible metaphor.

| Conditions | Tangible | Mouse | Tactile |
|---|---|---|---|
| Time | 8.7 s | 13.7 | 24.2 s |
| Ratings | 8 | 4 | 0 |

- **H1** & **H3** are validated

25. Zhai & Milgram, (1998) *CHI '98*

# Cutting plane

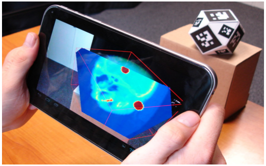

Task : Find the plane containing 3 red spheres in an IRM dataset.

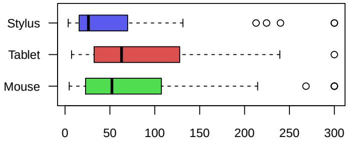


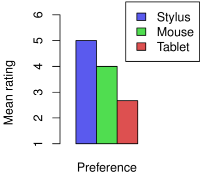


All these results are statistically significant ($p < 0.05$) in favor of the stylus metaphor.

| Conditions | Stylus | Mouse | Tablet |
|---|---|---|---|
| Time | 56 s | 79 s | 85 s |
| Ratings | 5 | 4 | 2.7 |

- **H2** & **H3** are validated

– Sensory threshold –

# Illusion from sensitivity

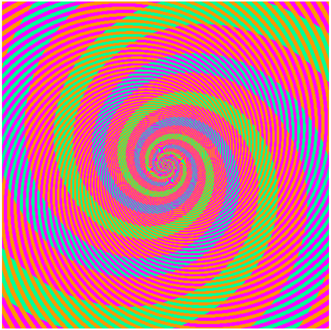

Green and blue branches share actually the same color.

# Illusion from sensitivity

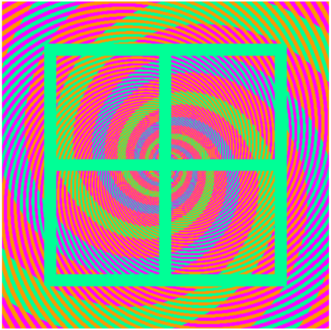

Green and blue branches share actually the same color.

# Illusion from sensitivity

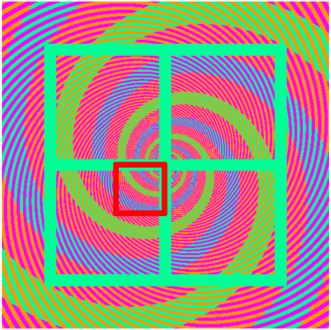

Green and blue branches share actually the same color.

# Illusion from sensitivity

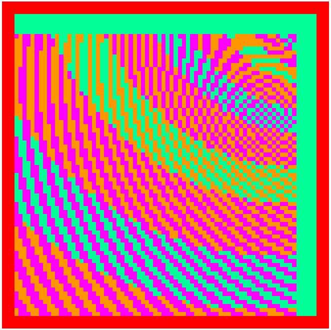

Green and blue branches share actually the same color.

# Sensory threshold

Identifying the threshold such as two stimulus are not perceived similarly by the user.

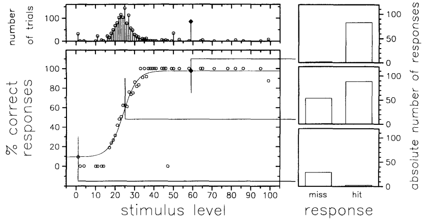


classical procedure [26]

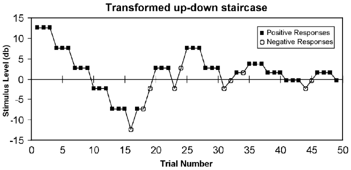


QUEST adaptative procedure [27]

26. Treutwein, (1995) *Visual Research*
27. Leek, (2001) *Perception and Psychophysics*

*"The stimulus domain has to be represented by a one-dimensional continuum."*

Bernhard Treutwein, (1995) *Vision Research*

# Sensory threshold for a 2D-dependant stimulus

Classical and adaptative algorithms are too time-costly for being used for determining the threshold when the stimulus is characterized by more than one parameter.

The main reason is potential miss-perception ("errors") of the stimulus by the subject.

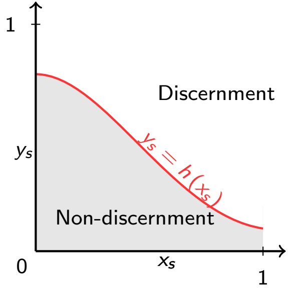


$x_s \equiv$ contrast

$y_s \equiv$ illuminance level

# A efficient method in multi dimensionnal stimulus

Statistical fit of the n-D threshold curve.

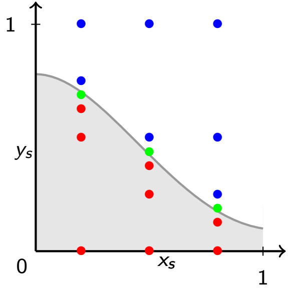


1. Determining points on the threshold curve
2. Identifying the curve by RMS fitting

## Numerical example

Despite the issue of subject's wrong answers, the convergence of the algorithm is still good.

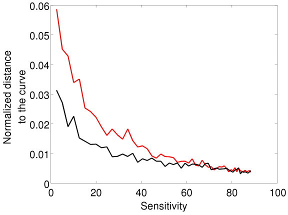


20 virtual participants

## Experimental illustration [EH2012]

A master curve is found for a 2D haptic stimulus.

$$\hat{f}(t) \propto f(t) + \cos\left(x_s \left(\frac{\mathrm{d}f}{\mathrm{d}t}\right)^{y_s}(t)\, t\right)$$

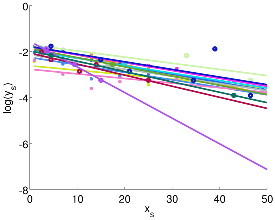


13 human participants

## Efficience of the 2D algorithm

| Method | QUEST | PEST | Dichotomy |
|---|---|---|---|
| Efficience (median) | / | / | 227% |
| Efficience (mean) | 84% | 45% | 1856% |

# – Conclusions –

# Conclusions

- Methods for extracting spectral informations of the dynamics, fitted for ill-conditionned dataset[1,2,3].
- Equation-free criterion for estimation the observability qualities of observable[3].
- Speed-up of FTLE field computations[4,5].
- Exploration of a cavity flow properties[2−6].
- Metaphors for interactive exploration of wide dataset[7,8].
- Algorithm for the identification of multi-dimensionnal sensory threshold[9].

# Future Works

- Minimization-free methods.
- Building a theoretical link between DMD decomposition (*i.e.* "Koopman operator") and Lagrangian structures (*i.e.* "Perron-Frobenius operator").
- Derive a theoretical framework around the DMD observability, and improve the criterion.
- So many things to do in SciViz !
- May a bayesian approach be possible for a multi-dimensionnal sensory threshold ?

# Publications

1. *POD-Spectral Decomposition for Fluid Flow Analysis and Model Reduction*, TCFD 2013
2. *Snapshot-Based Flow Analysis with Arbitrary Sampling*, ICTAM 2012
3. *DMD économique pour l'identification de structures dans des écoulements 3D*, RNL 2013
4. *Fast Identification of Lagrangian Coherent Structures*, BIFD 2011
5. *GPU and SIMD Acceleration for Identification of Lagrangian Coherent Structures. Application to an Open Cavity Flow*, BIFD 2013
6. *Lagrangian Coherent Structures in Open Cavity Flows*, ETC 2013
7. *A Design Study of Direct-Touch Interaction for Exploratory 3D Scientific Visualization*, EuroVis 2012
8. *Tangible Windows for a free Exploration of Wide 3D Virtual Environment*, VRST 2013
9. *Haptic Stimulus for the Discrimitation between Intrinsic Properties of Dynamic Systems*, EuroHaptics 2012

Thank you for your attentiveness.
If you have any questions, I will be pleased to answer them.

# – Annexes –

# – Cavity flow –

# Cavity flow : Experimental setup

- Cavity length : $L = 100$ mm
- Geometric ratio : $L/H = 1.5$,
- Incoming velocity : $U = 1.77$ m/s
- Dataset : $N = 5242$ velocity fields.
- $\mathrm{Re}_L = UL/\nu_{\mathrm{air}} = 8\,800$
- Dominant frequencies in the flow $St_L = fL/U \propto 1$ ($\approx$ 20Hz)
- Sampling frequency : 250 Hz

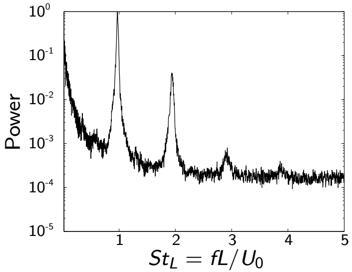

# Cavity flow : Experimental setup

- Cavity length : $L = 100$ mm
- Geometric ratio : $L/H = 2$,
- Incoming velocity : $U = 1.90$ m/s
- Dataset : $N = 4096$ velocity fields.
- $\mathrm{Re}_L = UL/\nu_{\mathrm{air}} = 12\,700$
- Dominant frequencies in the flow $St_L = fL/U \propto 1$ ($\approx$ 20Hz)
- Sampling frequency : 250 Hz

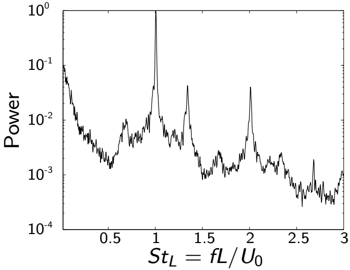

# Cavity flow : Experimental setup

- Cavity length : $L = 100$ mm
- Geometric ratio : $L/H = 2$,
- Incoming velocity : $U = 1.2$ m/s
- Dataset : $N = 1200$ velocity fields.
- $\mathrm{Re}_L = UL/\nu_{\mathrm{air}} = 8\,040$
- Dominant frequencies in the flow $St_L = fL/U \propto 1$ ($\approx$ 20Hz)
- Sampling frequency : 40 Hz

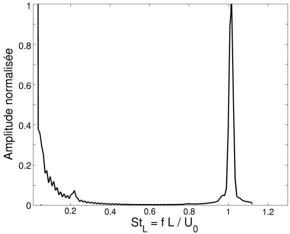

# Comparison DMD/POD

$\lambda_{POD}/L \simeq \frac{\gamma_1\lambda_1/L+\gamma_2\lambda_2/L}{\gamma_1+\gamma_2} = 0.44$

With $\gamma_1 = 1$ and $\gamma_2 = 0.67$

| | Strouhal | $\lambda/L$ |
|---|---|---|
| POD mode | 1.02 | $0.43 \pm 0.03$ |
| DMD mode $\mathbf{\Phi}_1$ | 1.02 | $0.49 \pm 0.03$ |
| DMD mode $\mathbf{\Phi}_2$ | 1.38 | $0.38 \pm 0.02$ |

# Comparison DMD/POD

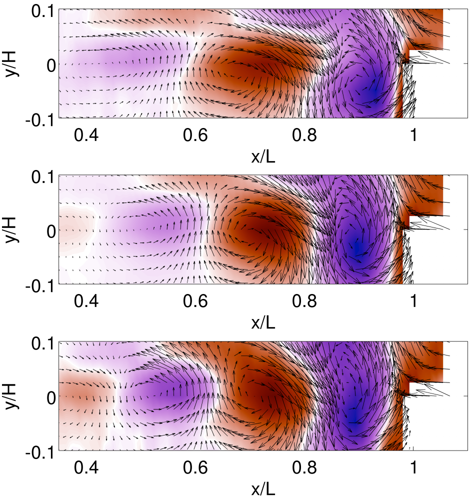

# Divergence

| Dynamic mode | $St_L$ | $S_{SL}/\alpha_0$ | $s_{IN}/\alpha_0$ | $S_{SL}/S_{IN}$ |
|---|---|---|---|---|
| $\mathbf{\Phi}_5$ | 0.028 | 3.4 | 5.7 | 0.6 |
| $\mathbf{\Phi}_3$ | 0.1 | 3.3 | 4.2 | 0.8 |
| $\mathbf{\Phi}_4$ | 0.3 | 3.5 | 3.6 | 1.0 |
| $\mathbf{\Phi}_1$ | 1.0 | 8.1 | 1.9 | 4.3 |
| $\mathbf{\Phi}_2$ | 1.4 | 11.9 | 1.7 | 7.1 |
| $\mathbf{\Phi}_0$ | 0 | 4.5 | 4.5 | 1.0 |

# Proper Orthogonal Decomposition

## A well-known method

We look for an orthonormal basis of spatial modes $\{\psi_i\}$, called *topos*[28] [29] , and temporal modes $\{\alpha_i\}$, called *chronos*, such as the average least-squares truncation error,

$$r_m = \sum_{k=0}^{t_N} \left\| \mathbf{u}\left(\mathbf{r}, t_k\right) - \sum_{i=0}^{m} \alpha_i\left(t_k\right) \psi_i\left(\mathbf{r}\right) \right\|,$$

Chronos and topos are obtained through an Singular Values Decomposition of the dataset.

28. G. Berkooz, P. Holmes, JL. Lumley, (1993), *Annu. Rev. Fluid Mech.*
29. M. Bergmann, L. Cordier, JP. Brancher,(2007), *NNFM*

# Link between DMD modes and with global modes

For a linear dynamics, $\phi$ is a matrix.

If the observable is the state vector ($\Pi = \mathcal{I}d$), in that case $A = \phi$.

Supposing that the operator $A$ is well-estimated, dynamical modes are global modes of the dynamics.

Otherwise, DMD modes are eigenmodes of an operator describing the saturated dynamics, with a possibly time-dependant flow.

# Data pre-conditioning

## Arnoldi method

$$
\begin{aligned}
AK_1^N &= K_1^N S \\
A(QR) &= (QR)S \\
AQ &= Q(RCR^{-1}) \\
AQ &= Q\tilde{S}
\end{aligned}
$$

$\tilde{S}$ is an Hessemberg matrix, moreover $\tilde{S}$ and $A$ are similar.

## Singular Value Decomposition

$$
\begin{aligned}
AK_1^N &= K_2^{N+1} \\
A(W\Sigma V^H) &= K_2^{N+1} \\
AW &= W\left(W^H K_2^{N+1} V\Sigma^{-1}\right) \\
AW &= W\hat{S}
\end{aligned}
$$

$\hat{S}$ and $A$ are similar.

# Spatial properties inheritance

Let consider a spatial linear operator applied to the observable :

$$\boldsymbol{\nabla} \cdot \mathbf{u}(\mathbf{r}, t) = 0$$

By injecting the modal decomposition :

$$\begin{aligned} \boldsymbol{\nabla} \cdot \mathbf{u}(\mathbf{r}, t) &= \boldsymbol{\nabla} \cdot \left(\sum_i \alpha_i(t)\, \boldsymbol{\Phi}_\mathbf{i}(\mathbf{r})\right) \\ &= \sum_i \alpha_i(t)\, \boldsymbol{\nabla} \cdot \boldsymbol{\Phi}_\mathbf{i}(\mathbf{r}) \\ &= 0. \end{aligned}$$

Then, remembering $\alpha_j(t)$ form an orthonormal basis, we have :

$$\begin{aligned} \int_{-\infty}^{\infty} \alpha_j(t) \sum_i \times \alpha_i(t)\, \boldsymbol{\nabla} \cdot \Phi_i(\mathbf{r})\, \mathrm{d}t &= \int_{-\infty}^{\infty} \sum_i \alpha_j(t) \times \alpha_i(t)\, \boldsymbol{\nabla} \cdot \Phi_i(\mathbf{r})\, \mathrm{d}t \\ &= \sum_i \boldsymbol{\nabla} \cdot \boldsymbol{\Phi}_\mathbf{i}(\mathbf{r}) \int_{-\infty}^{\infty} \alpha_j(t) \times \alpha_i(t)\, \mathrm{d}t \\ &= \boldsymbol{\nabla} \cdot \boldsymbol{\Phi}_\mathbf{j}(\mathbf{r}) \\ &= 0. \end{aligned}$$

Henceforward, as for the observable **u**, the divergence of each mode is zero.

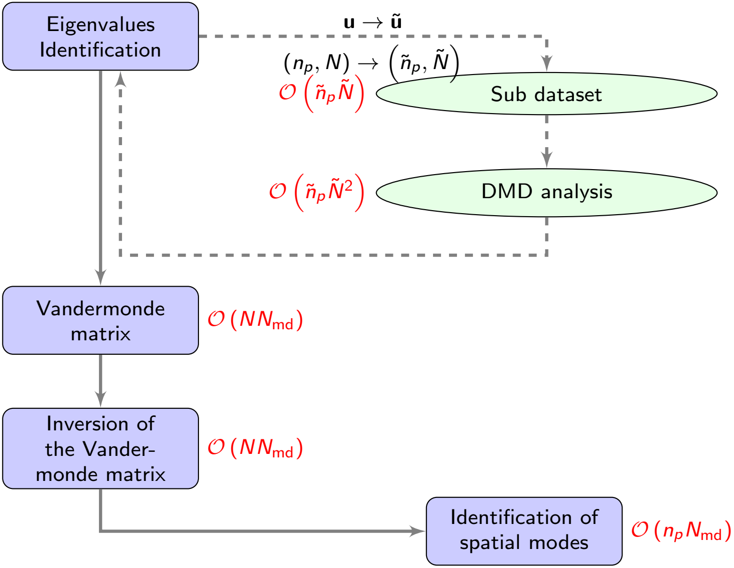
Eigenvalues Identification
$\mathbf{u} \rightarrow \tilde{\mathbf{u}}$
$(n_p, N) \rightarrow \left(\tilde{n}_p, \tilde{N}\right)$
$\mathcal{O}\left(\tilde{n}_p \tilde{N}\right)$
Sub dataset
$\mathcal{O}\left(\tilde{n}_p \tilde{N}^2\right)$
DMD analysis
Vandermonde matrix
$\mathcal{O}\left(N N_{\mathrm{md}}\right)$
Inversion of the Vandermonde matrix
$\mathcal{O}\left(N N_{\mathrm{md}}\right)$
Identification of spatial modes
$\mathcal{O}\left(n_p N_{\mathrm{md}}\right)$

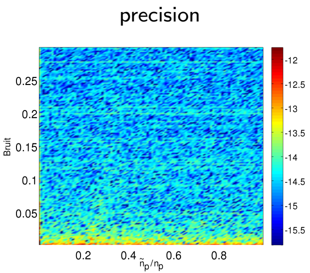
precision
Bruit
0.25
0.2
0.15
0.1
0.05
0.2
0.4
0.6
0.8
$\tilde{n}_p/n_p$
-12
-12.5
-13
-13.5
-14
-14.5
-15
-15.5

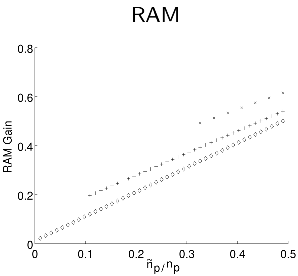
RAM
RAM Gain
0.8
0.6
0.4
0.2
0
0
0.1
0.2
0.3
0.4
0.5
$\tilde{n}_p/n_p$

# Annexes - Conformal transformations

Problem of the code : good only for regular mesh (for the SIMD)
Always true in experiences
Never true for DNS computations !
Solution : conformal transformations $\equiv$ ad hoc *inversible* deformation of the data.

$$\frac{\Delta \mathbf{x}_{conf}}{\mathbf{u}_{conf}} = \Delta t = \frac{\Delta \mathbf{x}}{\mathbf{u}}$$

# Annexes - Conformal transformations

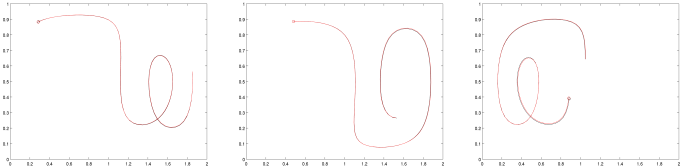

Some examples in a chaotic but synthetic flow.

# Illustration [BIFD2011,2013b]

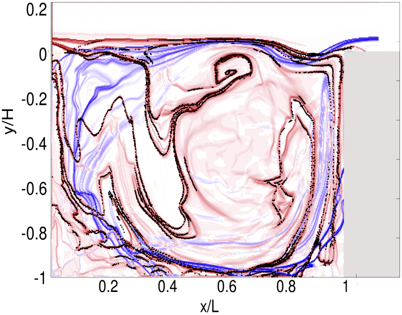


Black dots are virtual particles.

# Illustration [BIFD2011,2013b]

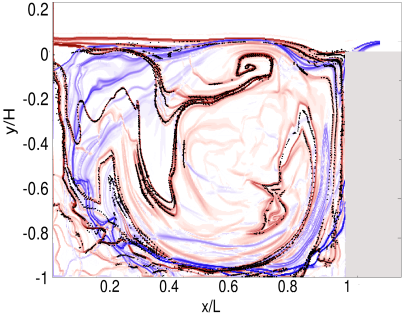


Black dots are virtual particles.

# Illustration [BIFD2011,2013b]

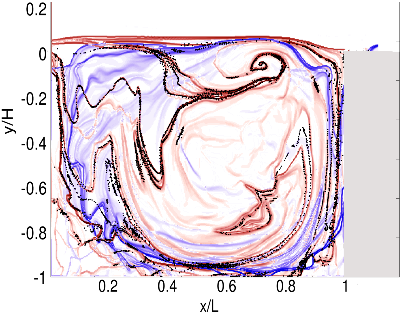


Black dots are virtual particles.

# Illustration [BIFD2011,2013b]

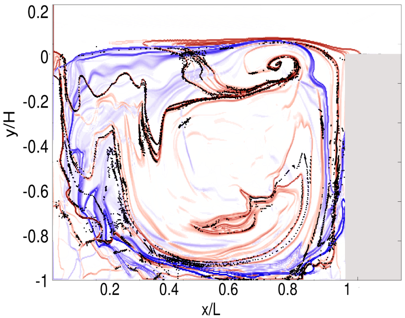


Black dots are virtual particles.

# Illustration [BIFD2011,2013b]

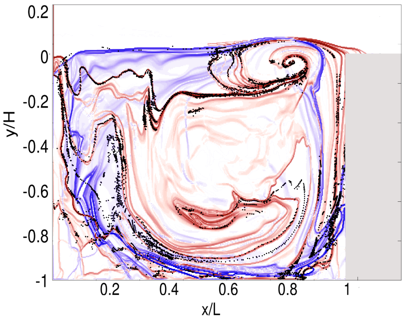


Black dots are virtual particles.

# Forward and backward LCS

## Qualitative results

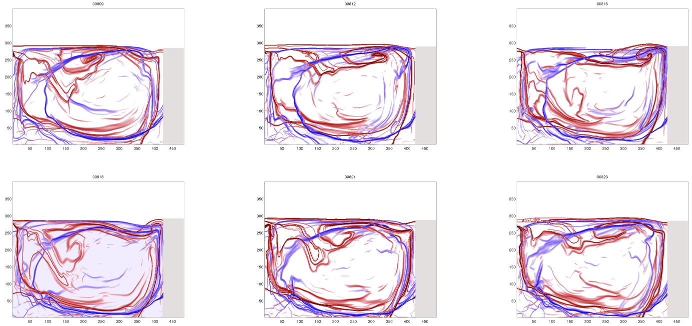

# Simplification of the flow

## DMD and Restricted Reduced Order Model

We build a synthetic flow, based on a Dynamical Modes Decomposition analysis of the dataset :

$$\mathbf{u}_{\mathbf{ROM}}(\mathbf{r}, t) = \bar{\mathbf{u}}(\mathbf{r}) + \mathcal{R}e\left(e^{i\omega t}\boldsymbol{\Phi}_{\omega}(\mathbf{r})\right)$$

where $\boldsymbol{\Phi}_{\omega}$ is the dominant shear layer DMD mode.
The periodicity of the model is important : Now one can see LCS structures as invariant manifolds in a Poincarré' section.

# Verification of relevance

## Comparison with real flows

ROM flow structures (top) and real flow structures (bottom), with similar horizon.

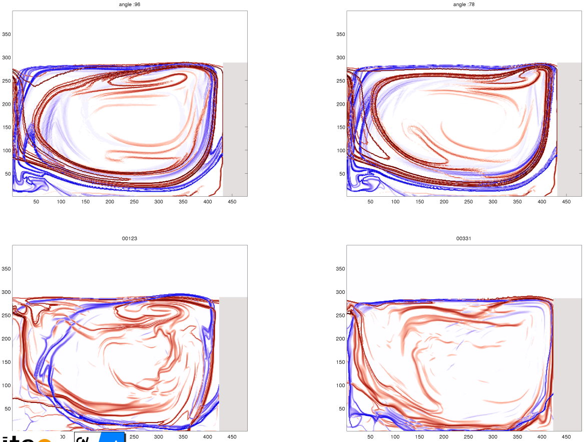

# Simplification of the flow (2/3)

## Invariant manifolds of the model

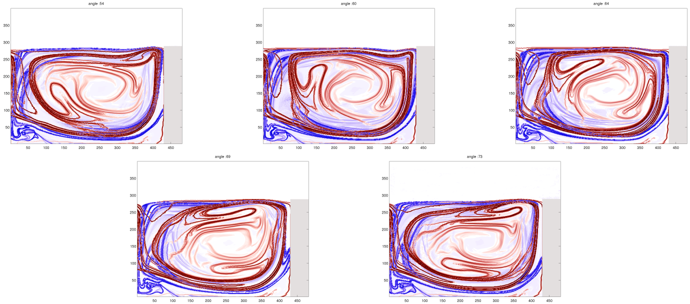

# Simplification of the flow (3/3)

## Horse-Shoes

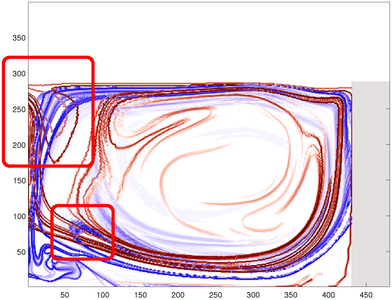

– DMD-Observability –

# Toy examples

If we take a synthetic matrix $A \in \mathcal{M}_n$, and a random vector $v \in \mathcal{M}_{n,1}$, we can construct a synthetic dataset :

$$K_1^N = \left\{ A \times v, A^2 \times v, \ldots, A^N \times v \right\}$$

# Toy examples

If $A$ is :

$$A = \begin{pmatrix} 1 & 0 & 0 & 1 & 1 \\ 0 & 1 & 0 & 0 & 0 \\ 1 & 0 & 1 & 1 & 1 \\ 0 & 0 & 0 & 1 & 1 \\ 1 & 0 & 0 & 1 & 0 \end{pmatrix}$$

then :

| Component : | 1 | 2 | 3 | 4 | 5 |
|---|---|---|---|---|---|
| Rank of $\mathcal{K}$ | 3 | 1 | 4 | 3 | 3 |
| $\sigma_{0.5}$ | 0.48 | 0.44 | 0.60 | 0.50 | 0.47 |

# Toy examples

If $A$ is :

$$A = \begin{pmatrix} 1 & 0 & 0 & 1 & 1 \\ 0 & 1 & 0 & 0 & 0 \\ 1 & 1 & 1 & 1 & 1 \\ 0 & 0 & 0 & 1 & 1 \\ 1 & 0 & 0 & 1 & 0 \end{pmatrix}$$

then :

| Component : | 1 | 2 | 3 | 4 | 5 |
|---|---|---|---|---|---|
| Rank of $\mathcal{K}$ | 3 | 1 | 5 | 3 | 3 |
| $\sigma_{0.5}$ | 0.56 | 0.30 | 0.64 | 0.49 | 0.51 |

# Parameters

*Hypothesis*
-**H1** : Subjects explore a larger space with the window metaphor
-**H2** : Finding a target takes less time with the window metaphor
-**H3** : Subjects prefer the window metaphor
*Conditions*
-**C1** : Use of the tangible window metaphor
-**C2** : Use of tactile metaphors
*Objective measurements*
-**MO1** : Number of eggs found over time
-**MO2** : Spatial displacement over time
-**MO3** : Angular displacement over time
*Subjective measurements*
-**MS1** : Rotating in the scene
-**MS2** : Finding eggs – Difficulty of the task
-**MS3** : Finding their way – Difficulty to self-localization

# Exploration

## A Significant improvement of the Exploration

Spatial displacement over time

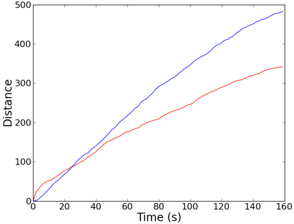


Angular displacement over time

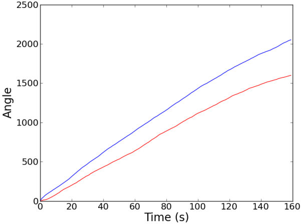


Both results are significantly ($p \ll 0.01$) in favor of the Window metaphor.

# Discussion on displacements

## A time-efficient metaphor

Activity (% of total time)

| | Condition **C1** | Condition **C2** |
|---|---|---|
| Rotation | 47.2% | 30.7% |
| Translation | 12.8% | 24.0% |
| Rotation + Translation | 11.2% | 4.80% |

| | Widget activation | Mean velocity | Motionless |
|---|---|---|---|
| Comparison **C1/C2** | +98% | +32.2% | −40.6% |

With the window metaphor, users travel more in the scene, in less time. They actually **know** where to go.

# Finding a target

## Mean time and main steps of the exploration

| | **C1** | Difference | p-value |
|---|---|---|---|
| Mean time | 70s | 24.4% | $p < 0.1$ |
| Fraction at $t_{c1} = 25$s | 8% | 0% | $p \gg 0.1$ |
| Fraction at $t_{c2} = 75$s | 65% | 39.1% | $p \ll 0.01$ |

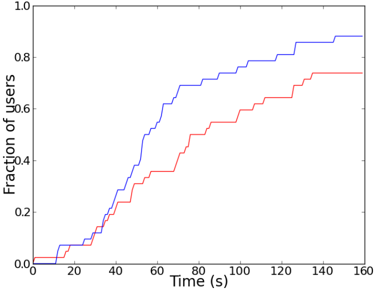

# Finding a target

## Mean time and main steps of the exploration

| | **C1** | Difference | p-value |
|---|---|---|---|
| Mean time | 70s | 24.4% | $p < 0.1$ |
| Fraction at $t_{c1} = 25s$ | 8% | 0% | $p \gg 0.1$ |
| Fraction at $t_{c2} = 75s$ | 65% | 39.1% | $p \ll 0.01$ |

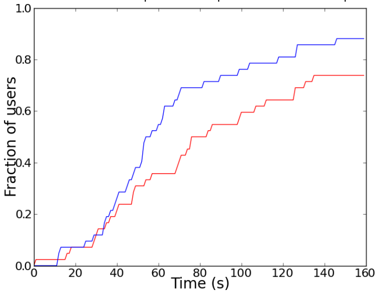

# Subjective measurements

-**MS1** : Rotating in the scene
-**MS2** : Finding eggs – Difficulty of the task
-**MS3** : Finding their way – Difficulty to self-localization

## A significant preference

| Measure : | MS-1 | | MS-2 | | MS-3 | |
|---|---|---|---|---|---|---|
| conditions | **C1** | **C2** | **C1** | **C2** | **C1** | **C2** |
| Median | 4.0 | 3.0 | 2.0 | 2.0 | 4.0 | 3.0 |
| p-value : | $p = 0.012$ | | $p \gg 0.05$ | | $p = 0.037$ | |

**MS-2** (difficulty of the task) was judge very hard, for both conditions. It was designed for being difficult, in order to force subjects to explore the scene.

Estimate the STD of parameters $x_s$ and $y_s$.

Without prediction correction

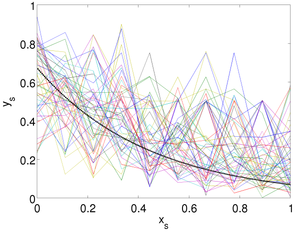


With prediction correction